

## INSTRUMENTATION OF HIGH PERFORMANCE CONCRETE BRIDGES

**David Knickerbocker**, Department of Civil and Environmental Engineering,  
Vanderbilt University, Nashville, TN  
**Prodyot K. Basu, DSc**, Department of Civil and Environmental Engineering,  
Vanderbilt University, Nashville, TN

### ABSTRACT

*Under FHWA's programs promoting the use of high performance concrete (HPC) in highway bridges, two double-span, jointless HPC bridges were thoroughly instrumented and tested during all phases of construction. Monitoring the performance of the bridges under environmental and operating conditions was continued for assessment of long-term effects. The results of the study verified some of the benefits of the use of HPC in practice, and have been presented to the highway bridge community. This paper is a detailed description of the instrumentation program used throughout the study.*

*Laboratory and field tests were performed for assessment of material properties, including compressive and tensile strength, elastic modulus, and chloride ion permeability. Systems were implemented to capture relevant values of deflection, strain, temperature, slope, and bridge movement. Particular instruments and their configurations that comprise these systems are described. In addition, the methods that were used to derive useful information from the collected data are reported. The success of the project was due in no small part to the viability of the instrumentation program. Room can always be found for improvement, and the lessons learned in this area are presented in interest of those performing similar work in the future.*

**Keywords:** High Performance Concrete Bridges, Bridge Instrumentation and Monitoring, Concrete Material Testing, Tennessee Department of Transportation

## INTRODUCTION

Increasing quality of feasibly produced structural materials holds promise for economical highway bridge construction and maintenance. This is evident in the rapidly expanding use of high performance concrete (HPC) in bridges. HPC is defined by the American Concrete Institute<sup>1</sup> as “*concrete meeting special combinations of performance and uniformity requirements that cannot always be achieved routinely using conventional constituents and normal mixing, placing, and curing practices*”. Characteristics of HPC generally include relatively high degrees of strength, long-term durability, and placeability; the desired properties of a particular HPC mix are achieved through high quality ingredients, including aggregates and specialized admixtures, and a low  $w/c$  (water to cementitious material) ratio.

For highway bridges, benefits of increased strength of HPC include longer maximum span lengths, decrease in required number of girders per span, and shallower superstructures. The benefit of longer spans goes hand-in-hand with fewer piers, leading to savings in substructure costs, and improved safety for under-passing waterway and highway traffic. Improved durability – especially against concrete deterioration mechanisms of freeze-thaw, scaling, abrasion, and chloride penetration – provides savings in life-cycle costs of maintenance and early replacement<sup>2</sup>.

For the potential benefits of HPC to highway bridge construction and maintenance, the Federal Highway Administration (FHWA) formed a national program to promote its use in highway bridges. The program sponsored construction and performance monitoring of “showcase” HPC bridges throughout the United States<sup>3</sup>. Under the program, and in cooperation with the Tennessee Department of Transportation (TDOT), two such showcase bridges have been built in Tennessee to assess performance and constructability under local conditions; namely, the Porter Road (PR) Bridge and the Hickman Road (HR) Bridge. The bridges take advantage of the strength of HPC, in that the equal-length, 159 ft (48.5 m) spans of the PR Bridge are the longest concrete bridge spans built as yet in Tennessee.

A research project was carried out by Vanderbilt University (VU) during construction and service stages to test materials, instrument the HPC bridge members, collect data on performance, and interpret and evaluate the results. As part of the effort it was necessary to study the practice of jointless bridge design and construction used predominantly in Tennessee, with especial reference to the two bridges in the study. The resultant findings have been reported<sup>4</sup>, and studies are underway toward gaining further insight into the behavior of jointless, continuous bridge structures<sup>5,6</sup>.

A topic of interest to the field of bridge engineers and researchers that has not yet been reported in detail is the instrumentation of the bridges in the above studies. This paper provides a detailed description of the instrumentation program implemented in the project. Forty-two vibrating wire strain gages were embedded in the girders and decks of each bridge, and eight removable digital tiltmeters were used in various locations. Systems were installed for measurement of camber and deflection, and longitudinal bridge movements. Details and rationale behind the program are provided, along with lessons learned during investigation of high performance concrete integral abutment bridges.

## DETAILS OF THE BRIDGES STUDIED

Both the Hickman Road Bridge and the Porter Road Bridge span across State Route 840 in Dickson County, TN. The two bridges, located roughly 35 miles southwest of Nashville, are jointless, making use of integral abutments with flexible pile supports to allow for superstructure movement, as per standard practice developed by TDOT. High performance concrete is used both in the precast prestressed girders and in the cast-in-place composite decks.

Requirements for compressive strength were set at 10 ksi (68.9 MPa) for prestressed girders, 5 ksi (34.5 MPa) for cast-in-place deck slabs, and 4 ksi (27.6 MPa) for substructure. Maximum permeability ratings by the rapid chloride ion permeability test<sup>7,8</sup> were specified as 1,500; 2,000; and 4,000 Coulombs for slab, girder, and substructure concrete, respectively. Minimum density of cement was specified as 658 lb/C.Y. (390 kg/m<sup>3</sup>) for both girder and deck HPC mixes. Also for both mixes, air content and slump were specified at 6±2% and 3±1 in (7.6±2.5 cm), respectively. Finally, maximum allowed *w/c* ratio for both mixes was set at 0.43. Mix designs for girder and deck concrete are summarized in Table 1, from which the design *w/c* ratios can be found to be 0.25 for girder, and 0.34 for deck concrete.

Table 1 Girder and Deck HPC Mix Designs

MIX:		GIRDER		DECK	
Materials		Density (U.S. Custom)	Density (Metric)	Density (U.S. Custom)	Density (Metric)
Fine Aggregate		974 lbs./yd <sup>3</sup>	578 kg/m <sup>3</sup>	1116 lbs./yd <sup>3</sup>	662 kg/m <sup>3</sup>
Coarse Aggregate	#67	1439 lbs./yd <sup>3</sup>	854 kg/m <sup>3</sup>	1810 lbs./yd <sup>3</sup>	1074 kg/m <sup>3</sup>
	#11	481 lbs./yd <sup>3</sup>	285 kg/m <sup>3</sup>		
Cement Type I		747 lbs./yd <sup>3</sup>	443 kg/m <sup>3</sup>	494 lbs./yd <sup>3</sup>	293 kg/m <sup>3</sup>
Flyash Type C		249 lbs./yd <sup>3</sup>	148 kg/m <sup>3</sup>	154 lbs./yd <sup>3</sup>	91 kg/m <sup>3</sup>
High-range water reducer		5-15 ozs./yd <sup>3</sup>	148-444 ml/m <sup>3</sup>		
Silica Fume				50 lbs./yd <sup>3</sup>	30 kg/m <sup>3</sup>
Water		29.75 Gals/yd <sup>3</sup>	147 l/m <sup>3</sup>	28 Gals/yd <sup>3</sup>	138 l/m <sup>3</sup>
Remarks:		<ul style="list-style-type: none"> <li>Retarder to be added when ambient temperature is 75°F or higher</li> <li>Maximum slump not to exceed 8 in. or 200mm after addition of high-range water reducer</li> </ul>		<ul style="list-style-type: none"> <li>Minimum <math>f_c' = 5,000</math> psi on field report of concrete specimen</li> </ul>	

Though reinforcement and prestressing details are somewhat different, the cross-sections of the superstructures are identical in overall dimensions. Four lines of precast prestressed (strand diameter = 0.6 in, or 15.2 mm) 72 in. (1.83 m) deep bulb-tee concrete girders, spaced on 100 in. (2.5m) centers, support a cast-in-place 8.25 in. (21.0 cm) deck slab. For pouring the 32 ft (9.75 m) wide deck, the gaps between girders are spanned by remain-in-place corrugated-steel-deck forms. The composite superstructure supports the cast-in-place parapet barriers, and all other superimposed dead and live loads. To resist the large negative moment over the pier support, adequate longitudinal steel is provided in the continuous deck.

The two-lane Hickman Road Bridge has an 18°-skewed substructure supporting two unequal spans of lengths 139.33 ft (42.5 m) and 151.33 ft (46.1 m). The roadway is on a mild vertical grade: 0.5%. The abutments are of similar size, with cross-sections measuring approximately 5 ft (1.5 m) deep by 9.5 ft (2.9 m) in height. Each girder of the shorter span is prestressed by forty-two strands, out of which four are debonded near the ends, and two are draped, or raised toward the ends of the girder. In the longer span, the girders are prestressed by fifty strands, 6 partially debonded and 6 draped.

The two-lane Porter Road Bridge has two equal spans of 159 ft (48.5 m) each with 27° skew. Unlike the Hickman Road Bridge, the two abutments differ significantly in size, with heights of 11 ft (3.4 m) and 3.5 ft (1.1 m). Each of the eight girders are pretensioned by fifty-four strands, out of which eight are debonded near the ends, and six are draped.

Following standard practice in Tennessee, the deck slabs were poured monolithically with the diaphragms over the piers, and with the backwalls. Continuity is thus developed just after maturity of deck concrete. Resistance to positive moment from creep and shrinkage of girders is provided by #5 (dia.=1.6 cm) rebars projecting from the girders into the diaphragms (or backwalls), and bent 90° upward. To increase the torsional stiffness of the superstructure, standard steel cross-bracing diaphragms are used in each span at third-points. The girders bear on 0.5 in. (1.3 cm) elastomeric pads. The intermediate bents are built after the style of semi-rigid piers – designed to allow rotation and partially resist translation of the superstructure. Piles supporting the abutments are placed in a single row along the skew to bend about the strong axis. These are embedded 1.0 ft (30.5 cm) into the abutment beams, with lengths varying according to geotechnical conditions. The backwall and two wingwalls serve to anchor the superstructure at each abutment.

## CURING

The quality of an HPC mix depends on many factors, including ingredients, mix proportions, and placement and curing practice. Curing practice for precast and cast-in-place members, and for the material test specimens, were observed and recorded. Methods of curing test specimens were varied in terms of curing temperature and ambient moisture. The details of curing practice and investigation involved in the project are outlined below.

## CURING OF PRECAST, PRESTRESSED GIRDERS

To accomplish detensioning strength as early as possible, the prestressed girders were steam-cured in the casting bed. As a result, measured internal concrete temperatures during hydration reached as high as 175°F (79°C), with average maximum recorded temperature at various locations of about 165°F (74°C). After concrete test cylinders were prepared, they were moved to their designated locations for initial curing. Most of the test cylinders were cast in steel molds (both 4 in. and 6 in. diameter specimen) and initially cured alongside the girders under the casting blanket. These were termed as “bed-cured” samples. The remaining girder concrete samples were prepared under match curing conditions, described below. Steam curing was performed for duration of 18-60 hours, depending on the manufacturing schedule. Usually, transfer strength was reached after the first 18-22 hours of curing, and the girders were then cut out and moved into storage. Precast, prestressed girders are required by Tennessee to remain free of encumbrance for a duration of 45 days so that the effects of shrinkage and creep may be largely undertaken before continuity is established in the bridge structure.

## PLACEMENT AND CURING OF CAST-IN-PLACE DECKS

The PR Bridge deck was placed in January with ambient temperatures ranging over 35 to 40°F (4°C). It was noted that, due to stickiness of the concrete mix, ridges formed perpendicular to the roadway. This phenomenon is a result of the motion of the screed pan, which tended to adhere to the concrete as it was swept back and forth across the deck surface. Also, it was noted that some pulling up of the aggregates did occur. These problems were attributed to lack of bleed water.

The HR Bridge deck was placed in May, when the temperature was about 70°F (21°C). Based on the experience gained from the PR Bridge deck placement, measures were taken to insure ample bleed water during the curing process. Extra fogging was used on the deck concrete until the slab could be covered with water-soaked burlap. Fogging refers to maintenance of moisture using pressure washers, introducing a mist over the deck surface. The size of the ridges that formed from the screed decreased, and the problem of aggregate pulling was eliminated.

Because of the more critical role of water in the curing process, moisture was maintained (with burlap) on the slab for 7 days rather than the usual 5. In general, it was noted that at high ambient temperatures, setting time is more rapid for HPC than for normal concrete. At low temperatures, a difference in curing time was not noticeable.

## EXPERIMENTAL CURING

It was of interest to make observations of the effects of varied levels of temperature and moisture in the curing process. Match curing during initial hardening stages was performed to observe any differences between conventionally cured samples, and those cured under the

same conditions as the structural concrete member. After the initial hardening stage, samples were cured in a “moist room”, in which a constant mist of water was maintained at room temperature. Finally, some samples were submersed underwater at 100°F throughout the curing process.

### Match-Curing

Match curing was accomplished by using the SURE CURE match-curing system manufactured by Products Engineering of Boulder, Colorado (see Fig. 1). The system consists of two major components: reusable one-piece 4-inch diameter by 8-inch cylinder molds, and a temperature-matching controller. The self-insulated mold has a built-in heating system and thermocouple temperature sensor that work in conjunction with the temperature-matching controller. Each temperature-matching controller can control the curing temperature in up to four cylinder molds at one time.



Fig. 1 Preparation of match-curing concrete batch material samples

The system is operated using a reference thermocouple, which is located in the actual concrete member to sense the temperature of freshly poured concrete, and connected to the controller along with the thermocouple from a cylinder mold. Power output cords from the controller plug into each cylinder mold to be cured. When the controller is operating, it continuously compares the referenced product temperature with the temperature of the

cylinder mold. When the product temperature exceeds the cylinder temperature, the controller energizes the heaters on the cylinder mold, thus causing the temperature of the test specimen to rise. Conversely, when the temperature of the cylinder mold reaches the product temperature, the controller interrupts the power to the cylinder heaters, thus allowing the test specimen to commence cooling.

The determination, provided by match curing, as to whether the test cylinders cure under the same conditions as the actual member is of substantial value. However, ensuring that this determination is valid can be difficult. The necessary match-curing equipment requires a much larger area of even landscape, which may not be available at close proximity on the job site. While above difficulties were encountered in match curing test cylinders from deck concrete, satisfactory results were obtained in match curing of girder concrete samples at the precasting yard.

## LABORATORY TESTING

It is always necessary to test the material properties of concrete batches used in a structure, to ensure that the structural design, based on assumptions of material properties, will be sufficient. In the research project, material testing was performed to satisfy these considerations, as well as to assess characteristics of HPC produced locally. Plastic concrete tests for slump and air content gave information on the placeability of the mix. Mechanical parameters of compressive strength, tensile strength, and modulus of elasticity were measured for characterization of the material, both for quality control, and for refinement of analytical studies. Finally, testing of chloride ion permeability was performed to assess chemical durability of the HPC, and to check material performance against the novel contract requirements,

## MECHANICAL PROPERTIES

Compressive strength was tested on “4x8” and “6x12” cylinders according to AASHTO T22<sup>7</sup> and ASTM C39<sup>8</sup>. Tests performed by VU were performed with a Forney compression testing machine, rated at 500,000 lbs. Extensive compressive strength testing was also performed by TDOT on all batches, and by CPI on girder batches. Assessments of tensile strength and modulus of elasticity were also performed at VU using the Forney compression testing machine on “4x8” cylinders. Tensile strength was measured according to the AASHTO T198<sup>7</sup> and ASTM C496<sup>8</sup> splitting tensile test. Modulus of elasticity testing was performed according to ASTM C469<sup>8</sup>.

## CHLORIDE ION PERMEABILITY

The tests for chloride ion penetration were performed in accordance with AASHTO Specifications T 277<sup>7</sup> and ASTM Specifications C 1202<sup>8</sup>. This test method consists of monitoring the amount of electrical current passing through two-inch thick slices of four-inch

nominal diameter cylinders during a six-hour period. The concrete specimen must be saturated with deoxygenated water and void of air, as this is the condition under which concrete is most vulnerable to chloride ion permeability. Specimen preparation requires the following procedure:

1. Specimen is sliced to 2-inch thickness by a circular wet saw, or brick saw.
2. Specimen is allowed to dry after cutting, silicone sealant is applied to circumferential surface, and allowed to cure.
3. Specimen is placed in a dessication tank, as shown in Fig. 2, for vacuum-removal of air from material.
4. After 3 hours of dessication, deoxygenated water is introduced into the dessicator, submerging the specimen, and dessication is continued for one hour more.
5. Specimen is sealed and stored in the submerged condition for 16-20 hrs.
6. Specimen is mounted in the test cells by sealing the circumferential boundaries between specimen edges and test cells. The specimen is then ready for testing.



Fig. 2 Pump system for the permeability cell

For a duration of 6 hours, a potential difference of 60 V DC is maintained across the ends of the specimen, one of which is immersed in a sodium chloride solution, the other in a sodium hydroxide solution; see Fig. 3. The total charge passed, in Coulombs, is related to the resistance of the specimen to chloride ion penetration<sup>7</sup>. Chloride ion penetrability based on the charge passed can be broken into five categories. Table 2 lists the categories and their corresponding Coulomb levels<sup>8</sup>.





Fig. 3 Permeability cell ready for test

To perform the chloride ion penetration tests, a RLC Instruments Model 164 testing machine was used; see Fig. 4. The machine gives the readouts for current and Coulombs for each specimen being tested (up to four at a time). The final Coulomb reading from the testing machine is then used in Eq. (1) below to obtain an adjusted value of the charge passed:

$$Q_s = Q_x \times \left( \frac{3.75}{x} \right)^2 \quad (1)$$

where  $Q_s$  is the charge passed (in coulombs) through a 3.75-inch standard diameter specimen and  $Q_x$  is the charge passed (in coulombs) through an  $x$ -inch diameter specimen. The value  $Q_x$  is read directly from the testing machine, with  $x = 4$  in. (diameter of the non-standard specimen).

Table 2 Chloride Ion Penetrability Based on Charge Passed<sup>8</sup>

Charge Passed (coulombs)	Chloride Ion Permeability
>4000	High
2,000-4,000	Moderate
1,000-2,000	Low
100-1,000	Very Low
<100	Negligible



Fig. 4 Setup for permeability test

## INSTRUMENTATION

For short-term and long-term evaluation of the behavior of the HPC, a program of bridge instrumentation was implemented. The instrumentation consists of sensors and devices to measure internal strain and temperature, camber and deflection, slope, and movement of the abutments. Within the configuration of bridge instrumentation outlined below are provided the ability to assess prestress losses in terms of curvature, axial strain, and mid-span deflection changes. Also, changes in strain and stress profiles due to changes in nonlinear thermal gradients are observable, along with the thermal gradient imposed by variable local conditions. Long-term effects of creep and shrinkage are quantifiable through the use of internal strain/temperature instrumentation. Furthermore, the effects of live load were measured in terms of slope, deflection, abutment movement, and internal strain profiles, which were instrumental in studies of distribution factors by calculation of moment in each girder.

Guidelines provided by the Federal Highway Administration<sup>9</sup> were followed in instrumentation of HPC bridges. The temperature and strain sensors were installed in girders and deck during the construction process. The instrumentation for camber and deflection measurements was installed immediately after the pretensioned girders were cast and again after the deck construction was completed. Instrumentation for slope and abutment movement measurements was undertaken after the completion of bridge construction.

## INTERNAL STRAIN AND TEMPERATURE

In order to monitor the response of the bridge (or its components) during construction and under operating conditions, it was necessary to measure strains in the girders and the deck at critical locations. As jointless construction was used it was also necessary to measure the temperature at critical locations of the bridge. The deck and two girders in each bridge were instrumented. In each of the instrumented girder sensors were located in three sections – near midspan and the two ends. The sensors in the deck were placed close to the instrumented girders. For long-term monitoring it was necessary to make these measurements at regular intervals over a long period of time. The volume and frequency of data collection required automation of the data acquisition system. For reliable data collection under the conditions of a construction site, it was necessary that the sensors and equipment used were robust without loss of accuracy. The choice of sensors and the data acquisition system were controlled by these factors.

### Strain Gages

An integrated temperature and strain measurement sensor, Model VCE-4200, manufactured by Geokon, Lebanon, New Hampshire, was used. This is a vibrating wire strain gage with a built-in thermistor to measure temperature, as shown in Fig. 5. Fourteen strain and temperature sensors were installed in each of the two instrumented girders for each bridge. In addition to the girder instrumentation, 14 gages were installed in the decks of each bridge, leading to a total of 42 sensors in each bridge. The method of operation, described in detail by Geokon in the Installation Manual<sup>10</sup>, is summarized below.

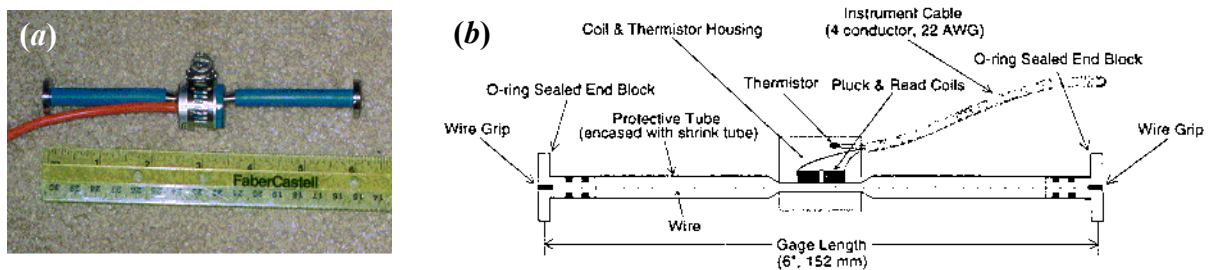


Fig. 5 (a) Geokon Model VCE-4200 Vibrating Wire Strain Gage; (b) Schematic of Inner Workings

Strains are measured using the vibrating wire principle: a length of steel wire is tensioned between two end blocks that are firmly in contact with the mass of concrete. Deformations in the concrete will cause the two end blocks to move relative to one another, altering the tension in the steel wire. This change in tension is measured as a change in the resonant frequency of vibration of the wire. Electromagnetic coils that are located close to the wire accomplish excitation and a readout unit captures the sensor frequency, which can be stored as data by using a data logger. It may be noted that the measured strain is actually the average of the strain over a gage length of 6". Thus it is not a pointwise measurement. The

location of the strain gage will be defined in terms of the location of its center point and the measured strains will accordingly be referred to the same point in the bridge.

The natural frequency of a wire of length  $L_w$ , cross-sectional area  $a$ , and material density  $\rho$  under an axial tension  $F$  is given by

$$f = \frac{1}{2L_w} \sqrt{\frac{Fg}{\rho a}} \quad (2)$$

in which acceleration due to gravity  $g = 386 \text{ in/s}^2$ . If the axial strain in the wire is  $\varepsilon_w$ , then Eq. (2) becomes

$$f = \frac{1}{2L_w} \sqrt{\frac{\varepsilon_w E g}{\rho}} \quad (3)$$

where modulus of elasticity for the wire material  $E = 30 \times 10^6 \text{ psi}$ .

As the gage length of the sensor  $L_g = 6''$ , is different from the length of the vibrating wire  $L_w = 5.875''$ , the change in length of wire should be equal to the change in gage length, and hence

$$\varepsilon_w L_w = \varepsilon L_g \quad (4)$$

in which  $\varepsilon =$  average strain of concrete over the gage length. It follows from Eqs. (3) and (4) that

$$\varepsilon = 4 \frac{\rho L_w^3}{E g L_g} f^2 \quad (5)$$

which is the relationship that allows the calculation of the concrete strain  $\varepsilon$  from a measurement of the resonant frequency of the wire  $f$ .

As gages are not manufactured as per the precise dimensions and properties specified, it is necessary to calibrate the gages after they are produced. This requires the definition of a gage calibration factor  $B$  that can be used in the formula for differential strain between stage  $i$  and  $j$  as shown in

$$\varepsilon_{j-i} = B(\varepsilon_j - \varepsilon_i) \quad (6)$$

As the coefficient for thermal expansion for the gage material and concrete are different, a correction should be applied to the strain readings for temperature changes between the two stages  $i$  and  $j$ . If the temperature at these two stages are  $T_i$  and  $T_j$  and the coefficients of thermal expansion for gage material and concrete are  $C_S$  and  $C_C$ , the strain differential after temperature change can be expressed as

$$\varepsilon_{j-i} = B(\varepsilon_j - \varepsilon_i) + (C_S - C_C)(T_j - T_i) \quad (7)$$

As long as the structure undergoes unrestricted thermal strain, the temperature effect will be corrected by Eq. (7). Otherwise, that is in the event of restraints against free thermal expansion that will create thermal forces, the reading will include the deformations associated with such thermal forces.

### Data Acquisition System

For continuous recording of strain and temperature data from all the sensors at regular intervals, automated data acquisition systems or dataloggers were used, one for each bridge. Model CR10X Dataloggers, manufactured by Campbell Scientific, Inc., Logan, Utah, and shown in Fig. 6, were used. Each datalogger could record temperature and strain signals from up to 48 sensors connected to it by low voltage wire. The temperature data is stored in the datalogger in degrees Celsius. The strain data is obtained by first measuring the natural frequency  $f$ , and Eq. (5) is then used to calculate the raw strain. The datalogger makes these calculations and stores the data in units of microstrain ( $\mu\varepsilon$ ). The final strain is then calculated on the basis of Eq. (7).

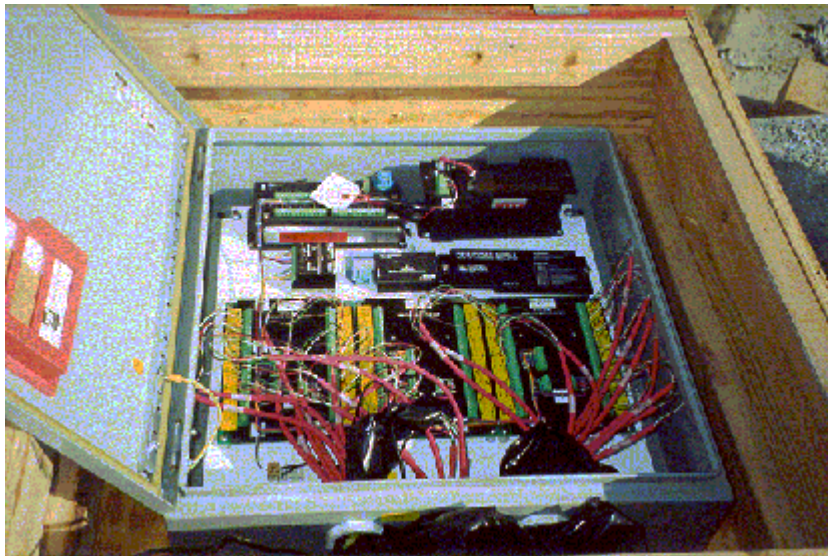


Fig. 6 Model CR10-X Datalogger

The datalogger can be set to acquire data at desired intervals of time, from a few minutes to one or more hours. The data stored in the logger could be downloaded at regular intervals, either manually by connecting a portable computer to it, or remotely by dialing in with a regular telephone modem, or by cellular phone link. For long-term data acquisition, a data-logging interval of 2 hours was chosen. This required downloading of data after about every four weeks, which happened to be about the same interval required for charging the batteries

in the datalogger using a portable generator. For these reasons, the option of monthly manual downloading of data was found to be more convenient and was adopted in this study. The dataloggers (one for each bridge) that read the sensor information use a convenient calendar system in which January 1, 2000 is 1/2000 and December 31, 2000 is 365/2000.

Installation in Girders

The same two girders in each bridge were instrumented for internal strain and temperature. These two girders form an “instrumented quadrant” of the superstructure, taking advantage of 2-way symmetry; see Figure 7(a). As seen from Figure 7(b), within one girder, vibrating wire strain gages with thermistors were embedded in three sections: at each end and at midspan. The process of placing the sensors in each girder required the construction of jigs, consisting of pieces of rebar welded in a configuration that allowed it to slide between the prestressing strands and stand in the middle of each girder cross section. Three jigs were prepared for each girder. The sensors were attached at pre-determined heights from the bottom of the girder cross section and then the jigs were inserted vertically down the middle of the girder sections.

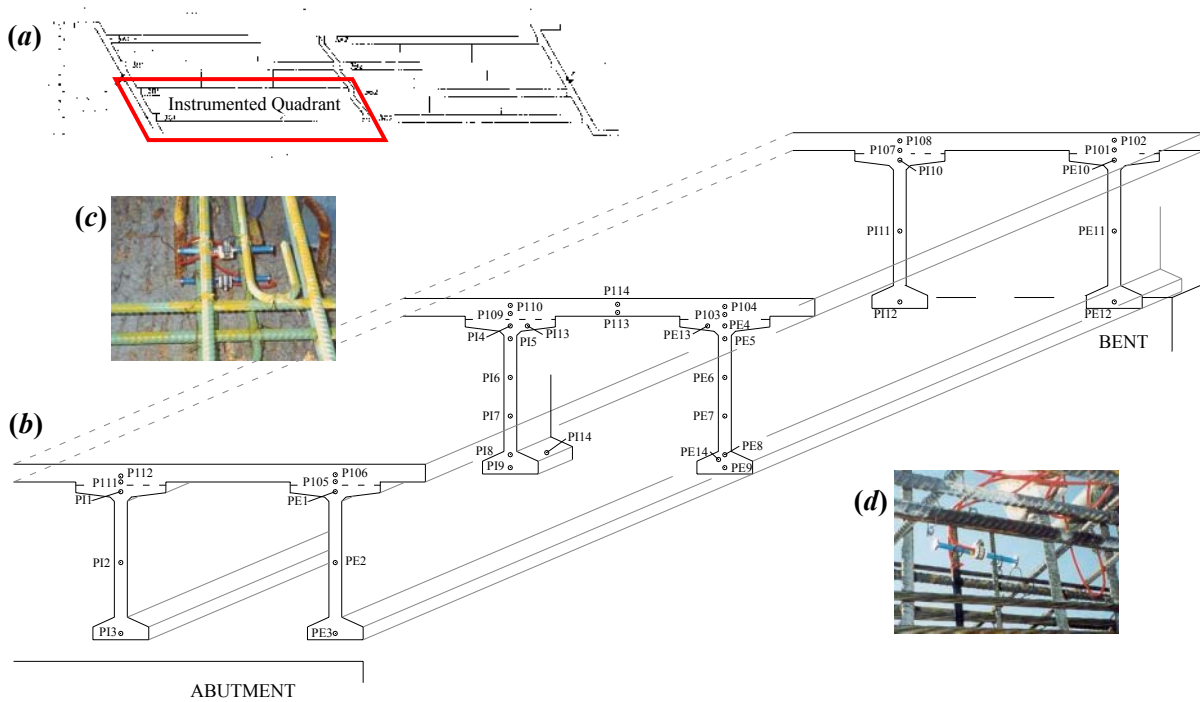


Fig. 7 – (a) Plan sketch of typical bridge showing instrumented quadrant; (b) locations of vibrating wire strain gages (with thermistors) within instrumented quadrant; typical installation in (c) deck, and (d) girder

Instrumented girders are denoted by, first P or H, for Porter or Hickman Road Bridge, and then by I or E, for interior or exterior. Instrumented sections are called by the girder notation, followed by a, c, or b, denoting location nearest the abutment, center-of-span, and

bent, respectively. Individual gages are also represented by the girder notation, and then followed by a location number, as presented in Figure 7(b). At an end section, three gages were placed about 6 ft (1.8 m) from the ends, at heights of 3", 36", and 69" (8, 91, and 175 cm). At midspan, six gages were placed at heights of 3",  $y_e$ , 27", 45", 63", and 69" (8,  $y_e$ , 69, 114, 160, and 175 cm), where  $y_e$  is the tendon centroid height (7" or 18 cm for H girders, 9" or 23 cm for P girders) at midspan. Two additional gages were placed at midspan in the top and bottom flanges.

### Installation in Decks

Two sensors were placed in the decks above each instrumented girder section, one near the top, and the other near the bottom of the deck slab. Typical installation is shown in Figure 7(d). In each bridge 14 sensors were installed in the deck, in addition to the 28 installed in the girders. After the installation of deck reinforcement was completed by the contractor, the gages were fastened near their ends to the rebar using soft iron tie wires, as recommended by Geokon.<sup>10</sup> Two sensors were placed above each instrumented section of the girder aligned with the center line of the girders. Thus, corresponding to six sections for the two instrumented girders in each bridge, twelve sensors were installed. An additional pair of sensors was installed at the center of the span and midway between the instrumented girders. The numbering of deck sensors begins with 101 and ends with 114. In the case of sensors used in PR Bridge deck, these numbers are preceded by the character P, and in the case of HR Bridge deck the corresponding character is H.

### Strain and Temperature Profiles

The temperatures recorded by the strain gage thermistors are used for heat of hydration and thermal loading studies; these are also used to apply thermal correction to the strain readings. Location of gages along the height of particular sections is useful for observation of thermal and strain gradients. Variation of strain can often be assumed linear, and the curvature can be estimated from these profiles as the slope of the least-squares fitting line. The corresponding moment is estimated by multiplying this curvature by stiffness,  $EI$ , of the section in question.

## CAMBER AND DEFLECTION

### Catenary Method

Camber measurements were undertaken for the test girders directly from the casting bed, immediately after prestress transfer. The subsequent camber measurement was undertaken with a string-pulley-weight system consisting of a weight ( $W = 14$  pounds) attached to a string weighing  $\omega = 0.001652$  pounds per foot (unstretched, clean, dry string). The string is supported by a screw near one end of the girder and by a pulley attached near the other end of the girder, as shown in Fig. 8. A ruler was affixed to the web of the girder at the midspan.

Every effort was made to ensure that the string line ran across the ruler but did not touch the girder or the ruler. Fig. 9 shows the weight/pulley, ruler, and the screw as used in the system for measurements in the storage yard.

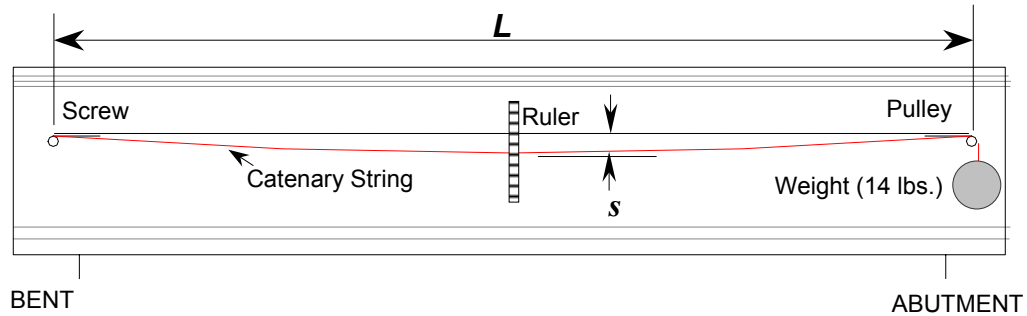


Fig. 8 String-Pulley-Weight Camber/Deflection Measuring System

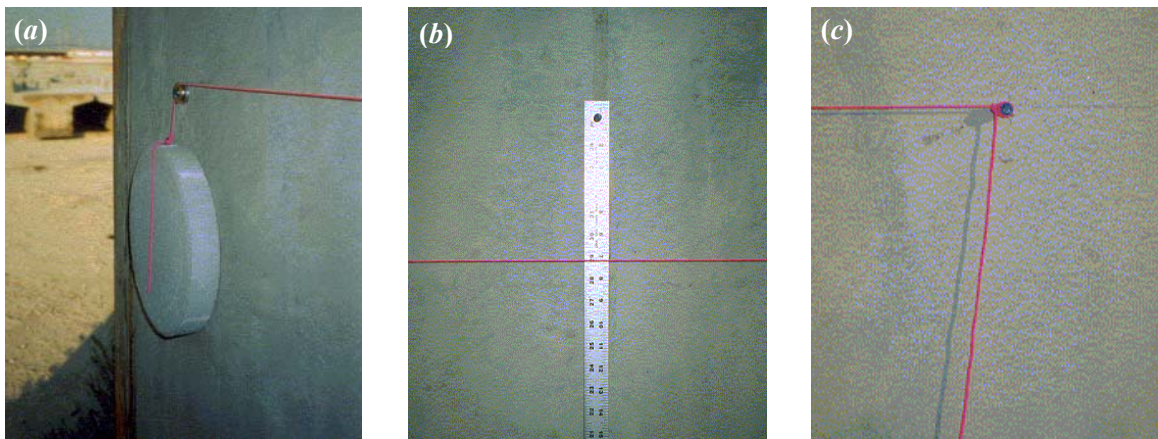


Fig. 9 (a) Pulley and Weight, (b) Midspan Ruler, (c) End Anchor

Under its own weight a stretched string hangs in the shape of a catenary with the maximum sag,  $s$ , given by the equation:

$$s = \frac{\omega L^2}{8H} \tag{8}$$

in which  $H$  equals the horizontal component of the tension in the string. Because the sag,  $s$ , is small relative to span  $L$  of the catenary, the horizontal component of the string tension can be taken with good approximation as the tension itself, which is the hung weight  $W$  (= 14 pounds), leading to:

$$s \approx \frac{\omega L^2}{8W} \tag{9}$$



This method may be prone to error for studying the long-term effects of the structure due to time-dependent properties of the string, disturbances caused by windy conditions, as well as the additional weight due to dust and grime accumulating on the string. These issues were somewhat mitigated by replacing the string with high strength piano wire, but a more broad-reaching solution was still desirable.

### Theodolite-Mounted Laser

To resolve the uncertainties with measurement of deflection by the taut-wire method, the HILTI model PD 20 laser range meter, shown in Fig. 10 (a), that measures distances from the unit to an arbitrary surface with acceptable accuracy, was procured. A housing was then machined to allow the range meter to be mounted in a theodolite, as in Fig. 10 (b) and (c), so that reference angles could be taken from a fixed, level location. The desired distance between two points, as in the example shown in Fig. 10 (d), could then be triangulated using the Law of Cosines:

$$A = \sqrt{B^2 + C^2 - 2BC \cos(\alpha)} \quad (10)$$

with distance measurements  $B$  and  $C$  from the unit to the two points, on the bottom of the girder and on the ground directly below, and measuring the angle  $\alpha$  between the two reference lines. For midspan deflection measurement, simple targets were mounted to ensure consistent measurement of the vertical distance. Extending the deflection measurement capability from the instrumented girders to all girders was then a simple matter of installing additional targets. This method has proven satisfactory for measuring deflections with acceptable accuracy at a much lower cost than more conventional surveying methods.

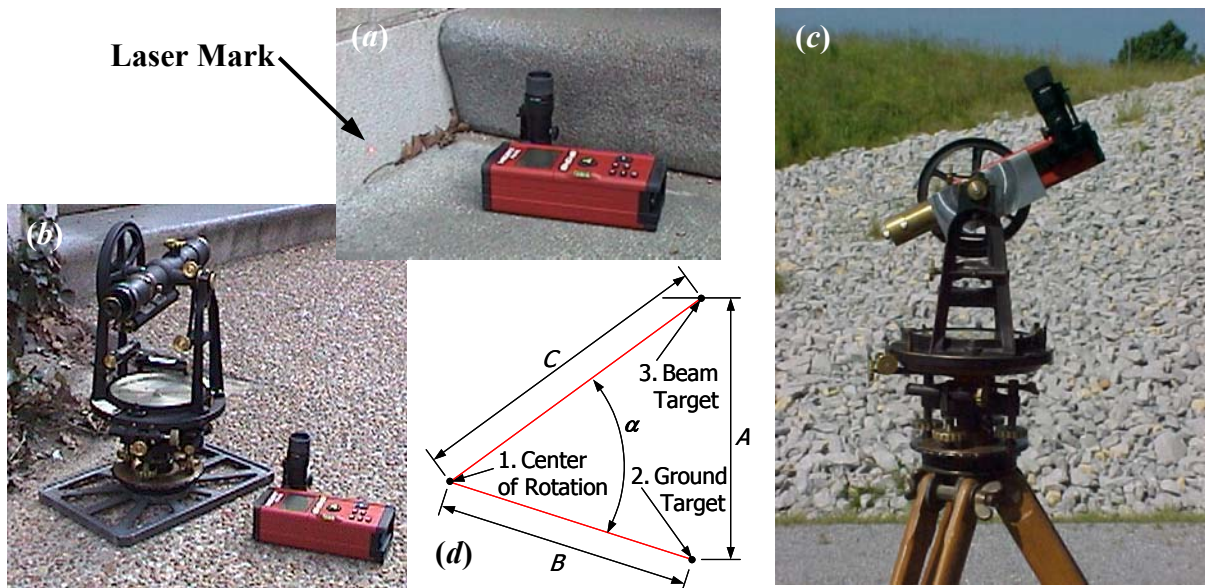


Fig. 10 (a) Laser range meter, (b) Range meter with theodolite, (c) Range meter mounted on theodolite (d) Deflection measurement using law of cosines

## SLOPE

To measure angular movements along the length of the bridge, eight tiltmeters Model 801-S manufactured by Applied Geomechanics, Santa Cruz, California were installed on the PR Bridge using mounting plates provided by Applied Geomechanics; see Fig. 11. The tiltmeters have a range of  $\pm 3^\circ$  with a resolution of  $0.0006^\circ$ . The tiltmeters were usually placed at the integral connections, and thus were particularly useful for studying the degree of continuity provided by the jointless construction. At some stages, especially during load testing of the bridge, the positions of the tiltmeters were changed. The lead wires of each tiltmeter were connected to a hand held readout module Model 870, also from Applied Geomechanics, with a digital voltmeter to obtain measurements of temperature and slope.



Fig. 11 Typical tiltmeter installation

## ABUTMENT MOVEMENT

Like the camber measurement system initially used, the method chosen for monitoring movement of the abutments was simple and straightforward. In this method, a steel “post” (rebar, diameter =  $1\frac{1}{2}$ ”) was set in concrete on each side of the abutment. The posts were exposed about 18” above the ground, =located about eight feet beyond the sides of abutment. The posts were placed so that a taut string, attached to the posts, would run parallel to the abutment face at a distance of about 6”. On each abutment wall, in level with the string, three reference points were fixed by concrete anchor screws. A sketch of this system is detailed in Fig. 13.

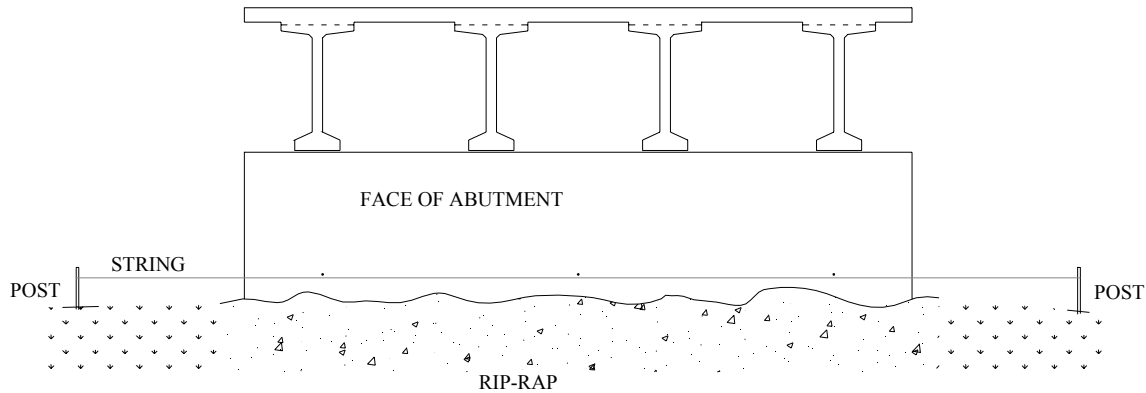


Fig. 13 Sketch of Abutment Movement Measuring System

## CONCLUSION

The HPC mixes used were investigated through extensive field and laboratory material testing. Properties of workability, strength, and durability were tested, and results were satisfactory, in terms of contract requirements met by local contractors. Two HPC bridges and their individual structural components have been instrumented for internal strain and temperature, slope, deflection and camber, and substructure movement. General observations of viability and methods of operation and data procurement have been described. The instrumentation program was successful due to advance planning and ready cooperation from the contractors. A great deal of insight was gained into the behavior of HPC in highway bridges, particularly in integral bridges per standard Tennessee DOT practice. In the interest of scope, collected data and analysis made possible by the material testing and instrumentation program described in this paper were not included. However, it has been presented and is available elsewhere.<sup>4</sup>

## REFERENCES

1. Russell, H. G. (1999). "From the Technical Activities Committee: ACI Defines High Performance Concrete." *Concrete International*, 21(2), 56-57.
2. Goodspeed, C. H., Vanikar, S., and Cook, R. A. (1996). "High Performance Concrete Defined for Highway Structures." *Concrete International*, 18(2), 62-67.
3. Miller, R. A. PCI Committee Report: High Performance Concrete Showcase Bridges. *PCI Journal*, Vol. 46, No. 6, November-December 2001, pp. 42-55.
4. Basu, P. K., and Knickerbocker, D. *High Performance Concrete Bridges*. TDOT Report TNSPR-RES1162. Department of Civil and Environmental Engineering, Vanderbilt University, 2002.
5. Knickerbocker, D. (2003) "Investigation of Integral Bridge Behavior by Finite Element Modeling." *Proceedings of the 20<sup>th</sup> Annual International Bridge Conference*. Pittsburgh, PA.

6. Basu, P. K., and Knickerbocker, D. "Discrete Numerical Modeling of Jointless High Performance Concrete Bridges." *Proceedings of the 3<sup>rd</sup> FHWA-PCI International Symposium on High Performance Concrete*. Orlando, FL.
7. AASHTO STANDARD SPECIFICATIONS FOR TRANSPORTATION MATERIALS AND METHODS OF SAMPLING AND TESTING: PART II TESTS-Nineteenth Edition. American Association of State Highway and Transportation Officials, Washington, DC, 1998.
8. ASTM Annual Book of Standards, Volume 4.02 Concrete and Aggregates. American Society for Testing and Materials, Philadelphia, PA, 1998.
9. Russell, H. G. *Implementation Program on High Performance Concrete – Guidelines for Instrumentation of Bridges*. Report FHWA-SA-96-075. FHWA, U.S. Department of Transportation, 1996.
10. GEOKON. (1996). *Installation Manual. Models VCE-4200/4202/4210 Vibrating Wire Strain Gages*. Geokon, Inc. Lebanon, NH.